

UCSF

Recent Work

Title

Variants in the CDKN2B and RTEL1 regions are associated with high-grade glioma susceptibility

Permalink

<https://escholarship.org/uc/item/32p785g8>

Author

Xiao, Yuanyuan

Publication Date

2009-07-08

Variants in the *CDKN2B* and *RTEL1* regions are associated with high-grade glioma susceptibility

Margaret Wrensch^{1,2,12}, Robert B Jenkins^{3,12}, Jeffrey S Chang^{4,12}, Ru-Fang Yeh^{4,12}, Yuanyuan Xiao⁴, Paul A Decker⁵, Karla V Ballman⁵, Mitchel Berger¹, Jan C Buckner⁶, Susan Chang¹, Caterina Giannini³, Chandralekha Halder³, Thomas M Kollmeyer³, Matthew L Kosel⁵, Daniel H LaChance⁷, Lucie McCoy¹, Brian P O'Neill⁷, Joe Patoka¹, Alexander R Pico⁸, Michael Prados¹, Charles Quesenberry⁹, Terri Rice¹, Amanda L Ryneerson³, Ivan Smirnov¹, Tarik Tihan¹⁰, Joe Wiemels^{2,4}, Ping Yang^{11,13} & John K Wiencke^{1,2,13}

The causes of glioblastoma and other gliomas remain obscure^{1,2}. To discover new candidate genes influencing glioma susceptibility, we conducted a principal component-adjusted genome-wide association study (GWAS) of 275,895 autosomal variants among 692 adult high-grade glioma cases (622 from the San Francisco Adult Glioma Study (AGS) and 70 from the Cancer Genome Atlas (TCGA))⁴ and 3,992 controls (602 from AGS and 3,390 from Illumina iControlDB (iControls)). For replication, we analyzed the 13 SNPs with $P < 10^{-6}$ using independent data from 176 high-grade glioma cases and 174 controls from the Mayo Clinic. On 9p21, rs1412829 near *CDKN2B* had discovery $P = 3.4 \times 10^{-8}$, replication $P = 0.0038$ and combined $P = 1.85 \times 10^{-10}$. On 20q13.3, rs6010620 intronic to *RTEL1* had discovery $P = 1.5 \times 10^{-7}$, replication $P = 0.00035$ and combined $P = 3.40 \times 10^{-9}$. For both SNPs, the direction of association was the same in discovery and replication phases.

Subject characteristics, including participation rates for the discovery GWAS and replication phases, are listed in **Supplementary Table 1a,b**. The distribution of P values from the principal component-adjusted logistic regression additive model across the genome for high-grade glioma cases versus controls (**Fig. 1**) suggests potentially meaningful associations for several SNPs on chromosomes 1, 5, 9, 11 and 20. **Supplementary Table 2** summarizes results for the 13 SNPs with $P < 10^{-6}$ for association with high-grade glioma in discovery data along with results from replication data; SNPs with Hardy-Weinberg $P < 10^{-5}$ in controls or with $> 5\%$ missing data in any case or control group were excluded. Three of these 13 SNPs (rs1412829 on 9p21, and rs6010620 and rs4809324 intronic to *RTEL1* on 20q13.3) had

significant association with high-grade glioma risk in the discovery phase (principal component analysis $P < 1.8 \times 10^{-7}$), were independent risk predictors in a multivariable analysis of 13 top hits, and were replicated in the Mayo Clinic dataset (**Table 1**). As shown in **Table 1** and **Supplementary Table 2**, the minor allele frequencies for the three SNPs consistently differed in the same direction between high-grade glioma cases and controls regardless of data source (AGS, TCGA, iControls or Mayo Clinic). **Supplementary Table 3** shows results from the multivariable model of discovery data that included all 13 SNPs (four from the 9p21 region, three in *RTEL1*, plus six others in other locations). Eight SNPs, including one in the 9p21 region and two intronic to *RTEL1*, remained independently associated with high-grade glioma risk after adjustment for other SNPs. This was expected given the strong linkage disequilibrium (LD) evident for the four 9p21 SNPs and two of the three *RTEL1* SNPs (**Supplementary Table 4**).

In discovery data, only the interaction between chromosome 9p21 SNP rs1412829 and *TERT* SNP rs2736100 on chromosome 5 was statistically significant with Wald test $P = 0.019$ (see **Supplementary**

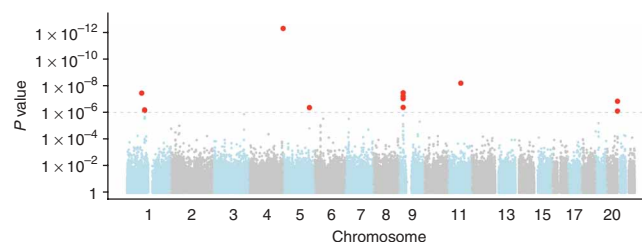


Figure 1 Distribution of P values from principal component-adjusted logistic regression additive model across the genome for high-grade glioma cases versus controls. The 13 SNPs with $P < 10^{-6}$ are shown in red.

¹Department of Neurological Surgery, University of California, San Francisco, San Francisco, California, USA. ²Institute of Human Genetics, University of California, San Francisco, San Francisco, California, USA. ³Department of Experimental Pathology, Mayo Clinic, Rochester, Minnesota, USA. ⁴Department of Epidemiology and Biostatistics, University of California, San Francisco, San Francisco, California, USA. ⁵Division of Biostatistics, ⁶Department of Oncology and ⁷Department of Neurology, Mayo Clinic, Rochester, Minnesota, USA. ⁸Gladstone Institute of Cardiovascular Disease, University of California, San Francisco, San Francisco, California, USA. ⁹Division of Research, Kaiser Permanente, Oakland, California, USA. ¹⁰Department of Pathology, University of California, San Francisco, San Francisco, California, USA. ¹¹Division of Epidemiology, Mayo Clinic, Rochester, Minnesota, USA. ¹²These authors contributed equally to this work. ¹³These authors jointly directed the work. Correspondence should be addressed to M.W. (margaret.wrensch@ucsf.edu).

Received 13 March; accepted 1 June; published online 5 July 2009; doi:10.1038/ng.408

Table 1 Three independent SNPs from the high-grade glioma discovery GWAS replicated in independent data from the Mayo Clinic

SNP	rs1412829	rs6010620	rs4809324
Chromosome	9	20	20
Position	22033926	61780283	61788664
Gene symbol		<i>RTEL1</i>	<i>RTEL1</i>
Minor allele	C	A	C
Discovery set: UCSF AGS and TCGA cases and AGS and iControls			
Number genotyped			
Cases	692	692	692
Controls	3,989	3,991	3,979
Minor allele frequencies			
Cases	0.47	0.17	0.15
Controls	0.39	0.23	0.10
Principal component-adjusted <i>P</i> value for cases versus controls	3.40×10^{-8}	1.50×10^{-7}	1.50×10^{-7}
OR and 95% CI for 0, 1 or 2 minor alleles	1.39 (1.24–1.57)	0.68 (0.58–0.79)	1.54 (1.31–1.82)
Replication set: Mayo Clinic glioblastoma and anaplastic astrocytoma cases and controls			
Number genotyped			
Cases	175	175	176
Controls	173	174	174
Minor allele frequencies			
Cases	0.53	0.15	0.16
Controls	0.41	0.26	0.10
Principal component-adjusted <i>P</i> value for cases versus controls	0.0038	0.00035	0.03
OR and 95% CI for 0, 1 or 2 minor alleles	1.56 (1.16–2.12)	0.48 (0.32–0.72)	1.66 (1.06–2.61)
Combined results			
Mantel-Haenszel combined <i>P</i> values	1.85×10^{-10}	3.40×10^{-9}	1.70×10^{-9}
OR and 95% CI	1.42 (1.27–1.58)	0.66 (0.57–0.76)	1.60 (1.37–1.87)

Principal component analysis implemented with EIGENSTRAT software. Complete results for 13 top hits with $P < 10^{-6}$ from UCSF GWAS and Mayo Clinic replication *P* values are shown in **Supplementary Table 2**, with Mantel-Haenszel combined results presented in **Supplementary Table 6**.

Table 5 and its accompanying graph). However, close inspection revealed that the interaction probably resulted from an association of the two SNPs in the controls.

P values of SNPs on 9p21 and the LD plot (**Fig. 2**) show that the top 9p21 SNPs are located in or around *CDKN2B*. Haplotype analyses (**Table 2**) showed that a single haplotype for the four 9p21 SNPs was more common in cases than controls. Two haplotypes in *RTEL1* were associated with increased and decreased risk, respectively (**Table 2**). The Mayo replication data also defined the identical haplotype associated with high-grade glioma risk for the four linked 9p21 SNPs as identified during the discovery phase (**Table 2**). In addition, one of the two *RTEL1* haplotypes identified in the discovery phase was also significantly associated in the replication samples (**Table 2**). Mantel-Haenszel combined *P* values for the UCSF and Mayo samples for the 13 SNPs are shown in **Supplementary Table 6**. The UCSF GWAS and Mayo replication suggest that regions of 9p21 (*CDKN2B*) and 20q13.3 (*RTEL1*) harbor SNPs associated with high-grade glioma risk, as discussed further below.

The strongest and most consistent associations in the GWAS were with a series of four SNPs within noncoding regions of the *CDKN2B* locus on 9p21. *CDKN2B* lies adjacent to the well-known tumor suppressor gene *CDKN2A* (encoding p16INK4A and p14ARF) in a region that is frequently mutated, deleted or hypermethylated in a wide variety of tumors, including high-grade glioma. The region is within 20 kb of constitutional deletions, including the hemizygous germline deletion of *CDKN2A* that has been reported by the Mayo group and others to be linked to familial melanoma and glioblastoma syndrome (**Fig. 2**)⁵. Mice with homozygous deletion of *Cdkn2a* and/or *Cdkn2b* are predisposed to develop tumors, including

gliomas⁶. *CDKN2B*, like *CDKN2A*, is a cyclin-dependent kinase inhibitor which forms a complex with CDK4 or CDK6 and prevents the activation of the cyclin-D-dependent kinases, thus regulating cell growth and cell cycle G1 progression. *CDKN2B* is frequently inactivated in glioma by homozygous deletion along with *CDKN2A*; 50–70% of primary high-grade gliomas show deletion of this region. Whereas tumor suppressor functions for *CDKN2A* have been firmly established, only recently has *CDKN2B* been recognized as an effective 'backup' for loss of *CDKN2A*⁷. In glioblastoma cells, overexpression of *CDKN2B* in a *CDKN2A*-deficient background inhibited cell growth, induced replicative senescence and inhibited telomerase activity⁸. In contrast to *CDKN2A*, *CDKN2B* is markedly induced by TGF- β . It has thus been hypothesized that *CDKN2B* may be engaged under special circumstances, whereas *CDKN2A* plays a more general tumor suppressor function in response to DNA damage and hyperproliferative signals⁸. TGF- β signaling information is relayed from the cell surface to the nucleus via the phosphorylation of SMAD proteins. A recent study identified a SMAD-binding region in the *CDKN2B* promoter; it is of interest that the SNPs associated with glioma in the current study are in LD with the rs2069418 G>C SNP that lies in the crucial conserved 3' box adjacent to the SMAD binding element⁹. If a SNP in this region reduces the responsiveness of *CDKN2B* to TGF- β , it could allow cancer precursor cell populations to expand, thereby promoting gliomagenesis. It is unknown, however, whether any SNP in the region can affect TGF- β or any other cytokine signaling processes.

Although recent studies^{10–13} have identified chromosome 9p21 as an important region for coronary artery diseases (CAD) and type 2 diabetes (T2D), the four glioma-associated chromosome 9p21 SNPs are not in LD with SNPs associated with CAD or T2D

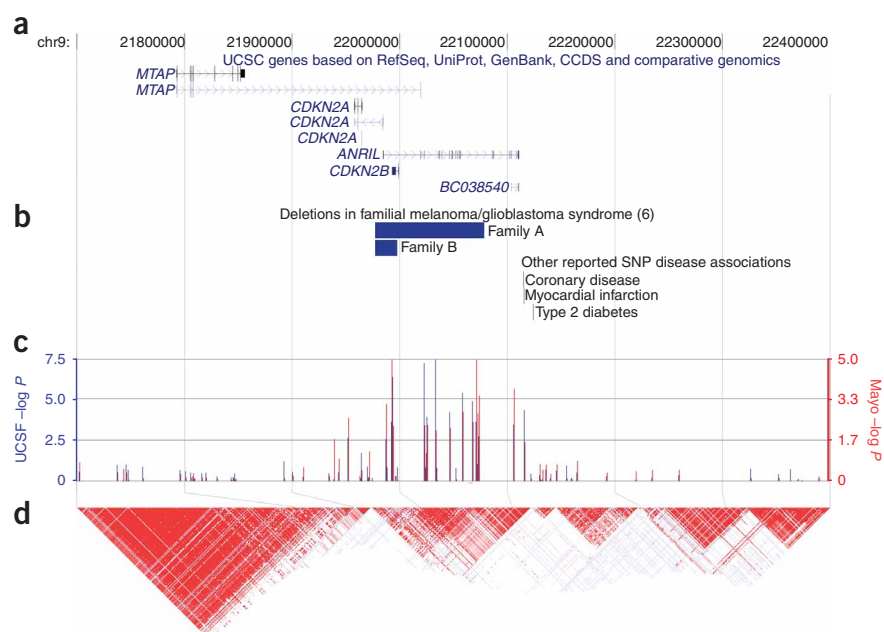


Figure 2 Map of the associated 9p21 region in high-grade glioma. **(a)** Genes within region. **(b)** Location of hemizygous deletion regions previously linked to familial melanoma/glioblastoma syndrome (blue)⁵. Also shown are SNPs within the region that have been previously reported to be associated with heart disease and diabetes risk¹¹. **(c)** $-\log P$ for SNPs within region; note different scales for UCSF discovery phase (blue bars, left x axis) and Mayo Clinic replication phase (red bars, right x axis). P values are from single point association tests of principal component-adjusted additive logistic regression of cases versus controls for 0, 1 or 2 minor alleles. **(d)** LD of HapMap SNPs in region.

idiopathic pulmonary fibrosis¹⁷. Another GWAS reported a significant association between *TERT* SNP rs2736100 and lung cancer¹⁸. On chromosome 20, we found that a related gene, *RTEL1*, contains two SNPs within intron 12 (rs6010620) and intron 17 (rs4809324) significantly associated with high-grade glioma. *RTEL1* is a DNA helicase critical

(Supplementary Fig. 1). This suggests that separate regions on chromosome 9p21 may contribute to the risk of high-grade glioma versus CAD and T2D.

Although replication results were not statistically significant, *TERT* is another interesting gene identified in our GWAS; it encodes human telomerase, which is a ribonucleoprotein polymerase that maintains telomere ends by addition of the telomere repeat TTAGGG. *TERT* activity is increased in glioblastoma^{14,15} and contributes to glioma cell growth¹⁶. A recent GWAS associated the region containing *TERT* with

for regulation of telomere length in mice, and its loss is associated with shortened telomere length, chromosome breaks and translocations¹⁹.

This study is strengthened by the use of principal components³ to adjust for any residual population stratification after using several quality control measures to assure that only unrelated subjects of European ancestry were included in the analyses (see Online Methods for details). Because glioma is a relatively rare disease, very large matched sets of glioma cases and controls are not currently available for GWAS. Consequently, we used a publicly available control group

Table 2 Haplotype analysis of associations of high-grade glioma risk with SNPs in the 9p21 region and *RTEL1*

	Cases (%)	iControls (%)	Odds ratio ^a	P value ^a
UCSF Adult Glioma Study (AGS) and the Cancer Genome Atlas high-grade glioma cases and AGS and Illumina controls				
Chromosome 9p21: rs1063192, rs2157719, rs1412829, rs4977756				
T-A-T-A	50.0	58.5	Referent	
C-G-C-G	43.2	35.1	1.42 (1.26–1.60)	1.4×10^{-8}
Rare haplotypes ^b	6.8	6.4	1.22 (0.96–1.56)	0.110
			Global P value ^a : 7.4×10^{-8}	
<i>RTEL1</i>: rs4809324, rs6010620, rs6089953				
T-G-G	68.0	66.9	Referent	
T-A-A	16.1	21.7	0.71 (0.61–0.83)	1.8×10^{-5}
C-G-G	15.0	10.3	1.40 (1.18–1.66)	9.6×10^{-5}
Rare haplotypes ^b	0.9	1.1	1.12 (0.57–2.19)	0.750
			Global P value ^a : 3.6×10^{-9}	
Mayo Clinic glioblastoma and anaplastic astrocytoma cases and controls				
Chromosome 9p21: rs1063192, rs2157719, rs1412829, rs4977756				
T-A-T-A	44.6	56.6	Referent	
C-G-C-G	49.7	36.5	1.68 (1.23–2.29)	0.001
Rare haplotypes ^b	5.7	6.9	0.96 (0.50–1.84)	0.900
			Global P value ^a : 0.002	
<i>RTEL1</i>: rs4809324, rs6010620, rs6089953				
T-G-G	68.1	63.2	Referent	
T-A-A	14.8	25.0	0.52 (0.35–0.79)	0.002
C-G-G	16.5	10.3	1.42 (0.89–2.26)	0.144
Rare haplotypes ^b	0.6	1.5	0.41 (0.08–2.22)	0.303
			Global P value ^a : 0.002	

^aPrincipal component-adjusted odds ratios, confidence intervals and P values were estimated using EIGENSTRAT software; SNPs with individual $P < 10^{-6}$ were included in the haplotype analyses.

^bRare haplotypes (<5%) were grouped together for these analyses.

from Illumina to provide large numbers of controls for the discovery phase. To minimize the possibility of false positives that might result from using a nonmatched control set, we used carefully matched high-grade glioma cases and controls from the Mayo Clinic for replication analyses. In summary, this report shows that high-grade glioma risk is associated with inherited variation in a region of 9p21 containing *CDKN2B* and a region of 20q13.3 tagged by two intronic SNPs in *RTEL1*. That the 9p21 region is frequently deleted in high-grade gliomas lends further biological plausibility to these findings.

METHODS

Methods and any associated references are available in the online version of the paper at <http://www.nature.com/naturegenetics/>.

Note: Supplementary information is available on the Nature Genetics website.

ACKNOWLEDGMENTS

Work at University of California, San Francisco (UCSF) has been supported by US National Institutes of Health grants R01CA52689 and UCSF Brain Tumor SPORE, P50CA097257, as well as by grants from the National Brain Tumor Foundation, the UCSF Lewis Chair in Brain Tumor Research and by donations from families and friends of J. Berardi, H. Glaser and E. Olsen. J.S.C. was also supported by a fellowship from the National Cancer Institute (grant R25 CA 112355). Work at the Mayo Clinic has been supported by the Mayo Clinic Brain Tumor SPORE (NIH P50 CA108961), the Mayo Clinic Comprehensive Cancer Center (P30 CA15083) and the Bernie and Edith Waterman Foundation. The San Francisco Adult Glioma Study thanks the Northern California Cancer Center for identifying glioma cases; we also thank K. Aldape for pathology review and the pathology departments of Alexian, Alta Bates, Brookside, California Pacific, Doctors Pinole, Eden, El Camino, Good Samaritan, Highland, John Muir, Kaiser Redwood City, Kaiser San Francisco, Kaiser Santa Teresa, Los Gatos, Los Medanos, Marin General, Merrithew, Mills Peninsula, Mt. Diablo Hospital, Mt. Zion, Naval Hospital, O'Connor, Ralph K Davies, Saint Louise, San Francisco General, San Jose, San Leandro, San Mateo County, San Ramon Valley, Santa Clara Valley, Sequoia, Seton, St. Francis, St. Luke's, St. Rose, Stanford, Summit, UC San Francisco, Valley Livermore, Veterans Palo Alto, Veterans SF, and Washington Hospitals and Medical Centers for providing tumor specimens for review. Genotyping services for San Francisco study subjects were provided by deCODE Genetics, Iceland. The company provided SNP and normalized CNV data and technical support in data analysis, including conference call tutorials in the use of the Disease Miner Software. We thank B. Scheithauer and C. Gianinni for their careful histological review of all the primary high-grade gliomas collected at the Mayo Clinic for this study. The Mayo Clinic Comprehensive Cancer Center Biospecimens and Processing (TACMA), Gene Analysis, Biostatistics and Bioinformatics Shared Resources were essential for the success of this study. We also thank K. Kelsey for helpful suggestions on genotyping and interpretation of results, N. Risch for very helpful suggestions on this paper and S. Sen for helpful discussions and suggestions on statistical methods. Some computations were performed using the UCSF Biostatistics High Performance Computing System.

AUTHOR CONTRIBUTIONS

M.W. was the overall UCSF study principal investigator who was responsible for subject recruitment, oversaw all analyses and wrote parts of and synthesized the paper. R.B.J. was the overall co-principal investigator of the Mayo study who oversaw the entire study (particularly laboratory quality control), interpreted the results and wrote parts of the paper. J.S.C. was the UCSF epidemiologist who contributed to development of the analysis plan, conducted statistical analyses and wrote parts of the paper. R.-F.Y. was the UCSF biostatistician who oversaw and conducted statistical analyses of the discovery phase and wrote parts of the paper. Y.X. was the UCSF biostatistician who conducted statistical analyses of the discovery and combined phases and wrote parts of the paper. P.A.D. was the Mayo statistician who performed all Mayo data analysis. K.V.B. was the Mayo lead statistician who participated in study design and the analysis plan. M.B. was the principal investigator of the UCSF Brain Tumor SPORE and a clinical collaborator who provided access for subject recruitment. J.C.B. was the Mayo neuro-oncologist who led subject recruitment. S.C. was the co-director of the UCSF neuro-oncology clinic who assisted in subject recruitment. C.G. was the Mayo pathologist who verified all pathologic diagnosis of Mayo cases. C.H. was the Mayo laboratory technologist responsible for specimen preparation for genotyping. T.M.K. was the Mayo laboratory manager responsible for specimen

storage and retrieval. M.L.K. provided statistical support for all Mayo analyses. D.H.L. was the Mayo neuro-oncologist who facilitated subject enrollment and medical record data collection. L.M. was the UCSF project coordinator responsible for subject recruitment and preparation of datasets for analyses, and also conducted analyses. B.P.O. was the principal investigator of Mayo brain tumor SPORE and neurologist who facilitated subject enrollment and medical record data collection. J.P. was the UCSF laboratory manager responsible for specimen storage, retrieval and preparation for genotyping. A.R.P. was the UCSF/Gladstone bioinformatician who participated in selecting the genotyping platform, developing the analytical plan and reviewing the paper. M.P. was the co-director of the UCSF neuro-oncology clinic who assisted in subject recruitment. C.Q. participated in subject recruitment and pathology specimen accrual from Kaiser Permanente Northern California. T.R. was the UCSF project coordinator responsible for subject recruitment, prepared datasets for analyses, conducted analyses and wrote parts of paper. A.L.R. was the Mayo project coordinator responsible for subject recruitment. I.S. was the UCSF bioinformatician who participated in developing the analytical plan, data analysis and interpreting results. T.T. was the UCSF neuropathologist who participated in subject identification, accrual and development of the analytical strategy. J.W. was the UCSF epidemiologist who participated in choice of genotyping platform and development of the analytical strategy and oversaw sample preparation. P.Y. was the overall co-principal investigator of the Mayo study who oversaw the entire study (particularly study design for subject recruitment, control enrollment, data quality control and analyses), interpreted results and wrote parts of the paper. J.K.W. was the UCSF study co-principal investigator who oversaw all aspects of laboratory work, participated in study design, subject accrual and development of the analysis plan, and wrote the discussion portion of the paper.

Published online at <http://www.nature.com/naturegenetics/>.

Reprints and permissions information is available online at <http://npg.nature.com/reprintsandpermissions/>.

1. CBTRUS. *Primary Brain Tumors in the United States, Statistical Report 2000–2004* (Central Brain Tumor Registry of the United States, Chicago, Illinois, 2008).
2. Schwartzbaum, J.A., Fisher, J.L., Aldape, K.D. & Wrensch, M. Epidemiology and molecular pathology of glioma. *Nat. Clin. Pract. Neurol.* **2**, 494–503 (2006).
3. Price, A.L. *et al.* Principal components analysis corrects for stratification in genome-wide association studies. *Nat. Genet.* **38**, 904–909 (2006).
4. Cancer Genome Atlas Research Network. Comprehensive genomic characterization defines human glioblastoma genes and core pathways. *Nature* **455**, 1061–1068 (2008).
5. Bahuau, M. *et al.* Germ-line deletion involving the *INK4* locus in familial proneness to melanoma and nervous system tumors. *Cancer Res.* **58**, 2298–2303 (1998).
6. Sharpless, N.E. *et al.* Loss of p16Ink4a with retention of p19Arf predisposes mice to tumorigenesis. *Nature* **413**, 86–91 (2001).
7. Krimpenfort, P. *et al.* p15Ink4b is a critical tumour suppressor in the absence of p16Ink4a. *Nature* **448**, 943–946 (2007).
8. Fuxe, J. *et al.* Adenovirus-mediated overexpression of p15INK4B inhibits human glioma cell growth, induces replicative senescence, and inhibits telomerase activity similarly to p16INK4A. *Cell Growth Differ.* **11**, 373–384 (2000).
9. Seoane, J. *et al.* TGF β influences Myc, Miz-1 and Smad to control the CDK inhibitor p15INK4b. *Nat. Cell Biol.* **3**, 400–408 (2001).
10. Lemmens, R. *et al.* Variant on 9p21 strongly associates with coronary heart disease, but lacks association with common stroke. *Eur. J. Hum. Genet.* advance online publication, doi:10.1038/ejhg.2009.42 (25 March 2009).
11. Mohlke, K.L., Boehnke, M. & Abecasis, G.R. Metabolic and cardiovascular traits: an abundance of recently identified common genetic variants. *Hum. Mol. Genet.* **17**, R102–R108 (2008).
12. Schaefer, A.S. *et al.* Identification of a shared genetic susceptibility locus for coronary heart disease and periodontitis. *PLoS Genet.* **5**, e1000378 (2009).
13. Schunkert, H. *et al.* Repeated replication and a prospective meta-analysis of the association between chromosome 9p21.3 and coronary artery disease. *Circulation* **117**, 1675–1684 (2008).
14. Shervington, A. *et al.* Glioma: what is the role of c-Myc, hsp90 and telomerase? *Mol. Cell. Biochem.* **283**, 1–9 (2006).
15. Maes, L. *et al.* Relation between telomerase activity, hTERT and telomere length for intracranial tumours. *Oncol. Rep.* **18**, 1571–1576 (2007).
16. Falchetti, M.L. *et al.* Telomerase inhibition impairs tumor growth in glioblastoma xenografts. *Neurol. Res.* **28**, 532–537 (2006).
17. Mushihiro, T. *et al.* A genome-wide association study identifies an association of a common variant in TERT with susceptibility to idiopathic pulmonary fibrosis. *J. Med. Genet.* **45**, 654–656 (2008).
18. McKay, J.D. *et al.* Lung cancer susceptibility locus at 5p15.33. *Nat. Genet.* **40**, 1404–1406 (2008).
19. Ding, H. *et al.* Regulation of murine telomere length by Rtel: an essential gene encoding a helicase-like protein. *Cell* **117**, 873–886 (2004).

ONLINE METHODS

Ethics. These studies were approved by the University of California San Francisco Committee on Human Research and Mayo Clinic Office for Human Research Protection. Informed consent was obtained from all study participants.

Study subjects for discovery phase. Genotyping data came from four groups of subjects: 622 high-grade astrocytic glioma cases and 602 controls from AGS, 3,390 controls from Illumina controls (iControls) and 70 glioblastoma cases from TCGA⁴ (**Supplementary Table 1a**) that passed quality control measures described below, including checks for relatedness and European ancestry. Details of subject recruitment for AGS have been provided previously^{20,21}. Briefly, cases aged 20 or older diagnosed with histologically confirmed incident gliomas (International Classification of Diseases for Oncology, morphology codes 9380-9481) were recruited from the local population-based registry, the Northern California Rapid Case Ascertainment program and the University of California, San Francisco Neuro-oncology clinic between 1997 and 2006. Additional pathology reviews were conducted by specialty trained neuropathologists. Glioblastoma, which is the diagnosis for the large majority (84%) of cases, is a diagnosis with good concordance between pathologists²². Although survival bias is a concern for studies of glioblastoma, we obtained blood from subjects within a median of 80 days from diagnosis. Nevertheless, the results may not apply to those with the most rapidly fatal forms of this disease. AGS controls aged 20 years or older from the same residential area as cases were identified using random digit dialing and were frequency matched to cases on age, sex and ancestry. Consenting participants provided blood and/or buccal specimens and information during an in-person or telephone interview. Because of the large-scale genotyping platform used, only subjects who provided blood specimens were included in the present analysis. We initially only included individuals who self-identified as white in the genotyping, but then used methods described below to verify European ancestry.

We also assembled an independent control genotype dataset of 3,390 nonredundant European-ancestry controls from Illumina iControlDB. The subjects are anonymous, with information only on their age, sex and ancestry. The iControl data also included 262 HapMap samples (30 CEU parent-child trios (Utah residents with ancestry from northern and western Europe), 84 YRI (Yoruba in Ibadan, Nigeria) and 88 Chinese or Japanese) that we used to identify and remove subjects with evidence of non-European ancestry from our analysis. We checked for evidence of non-European ancestry (**Supplementary Fig. 2**) and sample duplicates or related subjects (IBS > 1.6; **Supplementary Fig. 3**) among AGS samples, TCGA and iControls by performing multi-dimensional scaling (MDS) analysis on 20 bootstrap samples of 1,000 random autosomal biallelic SNPs. Following these quality assessment measures, we obtained a total of 3,390 European-ancestry controls from three different Illumina panels with up to 306,154 autosomal SNPs overlapping the HumanHap370duo panel used for the AGS subjects: Illumina HumanHap300 ($n = 336$ subjects), HumanHap550v1 ($n = 1,519$) and HumanHap550v3 ($n = 1,552$).

We downloaded HumanHap550 platform genotyping data from blood specimen DNA and demographic data for 89 glioblastoma cases from the Cancer Genome Atlas (TCGA)⁴. Although 72 were identified as white, our analyses showed that one had non-European ancestry (**Supplementary Fig. 3**) and another appeared to duplicate an AGS case, leaving 70 TCGA cases.

Sample preparation and genotyping for discovery phase and quality control.

DNA was isolated from whole blood using Genra Puregene DNA isolation kit (Qiagen) and quantified using Picogreen reagent (Invitrogen). Genotyping was conducted by deCODE Genetics. Samples were randomized before plating on specimen plates provided by deCODE Genetics. The genotyping assay panel used was Illumina's HumanCNV370-Duo BeadChip. For this paper, we only analyzed autosomal SNPs. A complete list of the SNPs on this panel is available either from Illumina or on the publicly available website of SNPLogic²³. In addition to randomization of samples and the quality control measures provided by deCODE Genetics, we included two duplicate samples per plate and one CEPH²⁴ trio (parents and child) per plate. DNA was re-extracted for any samples with call rates <98% and genotyped again and only samples reaching call rate $\geq 98\%$ were included in these analyses. We genotyped a total of 1,403 samples including AGS high-grade glioma cases ($n = 623$) and

controls ($n = 602$), duplicates ($n = 51$), some subjects that were determined to be ineligible based on self-described ancestry ($n = 22$), AGS cases with non-high-grade glioma histologies ($n = 67$) and CEPH samples we provided for quality control ($n = 36$); one sample was deleted because of inadequate call rate and one because of a mismatch between stated and genotyped sex. In addition, one case subject was removed because of not clustering with those of European ancestry in the identity-by-state (IBS) analysis (**Supplementary Fig. 2**). Thus, we used genotyping data from 622 AGS high-grade glioma cases and 602 AGS controls (**Supplementary Table 1a**).

The assay panel contained a total of 370,404 probes, of which 353,202 were associated with a reference sequence number and 17,202 with a copy number variant. There were a total of 342,554 SNPs provided in the genotyping files received from deCODE, with 331,697 autosomal SNPs. Of these, 250 had completely missing data and 4,941 were nonpolymorphic; this left 326,506 biallelic SNPs for analysis.

Quality control information for AGS cases and controls is presented in **Supplementary Figures 4, 5 and 6** showing autosomal heterozygosity for all 1,403 genotyped samples, percent of SNPs missing in cases versus controls, and Hardy-Weinberg equilibrium P values for AGS cases versus AGS controls. We used this information to exclude SNPs with poorer data quality from presented data. Similar quality measures were computed and used for filtering iControl and TCGA data (data not shown). After excluding SNPs with $P < 10^{-5}$ for Hardy-Weinberg equilibrium in either AGS controls or iControls and those with >5% missing genotyping data in any of the four subject groups, AGS cases or controls, iControls or TCGA cases, there were 275,895 SNPs to consider in case-control association tests.

In addition to ancestry checks described above, we ran EIGENSTRAT³ to adjust for other possible population or batch differences between the combined high-grade glioma cases and control groups. The quantile-quantile plot (**Supplementary Fig. 7**) for the EIGENSTRAT-adjusted P values comparing AGS and TCGA cases versus AGS and Illumina controls showed good correspondence between observed and expected test P values for equality of allele frequencies for the vast majority of the SNPs except for the ones with very low P values. The genomic control parameter, 1.058, was very similar to that found by Hung *et al.*²⁵ of 1.03. They interpreted this to indicate there was no systematic increase in false-positive findings owing to population stratification or any other form of bias. We also present the quantile-quantile plot comparing principal component-adjusted P values for AGS versus Illumina controls (**Supplementary Fig. 8**). The genomic control parameter for this comparison is 1.07.

Statistical methods for discovery phase. We used three software packages to conduct all analyses: R, Disease Miner (deCODE genetics) and EIGENSTRAT³. We also used Microsoft Excel and SAS for additional data manipulations and visualization. As noted above, quality control analyses included computation of sample heterozygosity, percent missing data (no genotype call) and Hardy-Weinberg equilibrium. The primary analyses used in this paper were EIGENSTRAT-adjusted single point association results from the additive logistic regression model for 0, 1 or 2 copies of the minor allele (equivalent to a Cochran-Armitage test for trend). We used a two-stage statistical approach to identify SNPs independently associated with high-grade glioma and potential SNP-SNP interaction effects. In the first stage, a backward selection procedure was used to obtain the best logistic regression model, using the 13 SNPs that produced a P value < 10^{-6} in the single locus models. Eight SNPs remained in the model after the backward selection procedure, suggesting a significant and independent association with high-grade glioma risk, among which one 9p21 SNP (out of four) and two *RTEL1* SNPs (out of three) were retained (**Supplementary Table 3**). Having confirmed significant main effects for these eight SNPs, we investigated in the second stage whether there are SNP-SNP pairwise interactions among them. This was performed again in a backward selection logistic regression framework using the eight SNPs and all pairwise interactions among them as covariates. Only the interaction between the 9p21 SNP rs1412829 and *TERT* SNP rs2736100 was statistically significant with $P < 0.05$ (Wald test) after backward selection. In **Supplementary Table 5**, we calculated ORs of the nine genotype groups of rs1412829 [TT,CT,CC] and rs2736100 [GG,GT,TT] using [rs1412829 = TT, rs2736100 = GG] as a referent group. Because the resulting P values are subject to multiple

testing errors, we also provide Bonferroni-adjusted P values. For the top hits, we also conducted sensitivity analyses using logistic additive regression models adjusting for age and sex (data not shown).

Haplotype analyses for the chromosome 9 and *RTEL1* SNPs were carried out using the haplo.stats R package. Rare haplotypes (<5%) were combined into one group for analysis. Global P values were calculated to assess whether any one of the haplotypes was over- or underrepresented among cases compared to controls. Haplotype trend regression was conducted to calculate OR associated with each copy of a specific haplotype using the most frequent haplotype as the referent group (Table 2). LD (r^2) among the four significant 9p21 SNPs and three significant *RTEL1* SNPs was calculated using PROC ALLELE procedure in SAS Genetics. A LD plot (Supplementary Fig. 1) showing the linkage pattern in r^2 between our four 9p21 glioma-associated SNPs and seven CAD or T2D SNPs^{10–13} was constructed using Haploview²⁶ with HapMap data of European ancestry (CEU). As shown, none of the four glioma-associated SNPs (rs1063192, rs2157719, rs1412829, rs4977756 at positions 21993367 to 22058652) shows any marked LD with seven CAD- or T2D-associated SNPs (rs2891168, rs1333042, rs2383206, rs10757278, rs1333048, rs1333049, rs2383208 at positions 22088618 to 22122075), with maximum $r^2 = 0.47$ between rs4977756 and rs2891168. For rs1412829, the 9p21 SNP independently associated with glioma risk in multivariate analysis, the maximum correlation with the CAD- or T2D-associated SNP (rs2891168) was $r^2 = 0.23$.

For completeness for other glioma genetics researchers, we also present SNP-disease association data for any SNP with $P < 0.001$ for tests of associations with high-grade glioma (Supplementary Table 7). We also conducted all analyses on glioblastoma only cases; no major differences for statistically significant SNPs were found (data not shown).

To obtain combined estimates of high-grade glioma risk for top SNPs from UCSF and Mayo, we used the Mantel-Haenszel method to estimate the OR, 95% CI and P value; the test is for equality of allele frequencies between cases and controls.

Subjects for replication phase. The Mayo Clinic case group included 176 individuals with glioblastoma and anaplastic astrocytomas newly diagnosed between 2005 and 2008. Cases were identified within 24 h of diagnosis, except for those who had their initial diagnosis elsewhere, followed by verification at the Mayo Clinic. The cases consisted of 67 (38%) women and 109 (62%) men who were 53.8 ± 12.6 years old; 174 (98%) were white; 114 (65%) had glioblastoma; 62 (35%) had anaplastic astrocytomas. Pathologic diagnosis was confirmed by review of the primary surgical material for all cases by two Mayo Clinic neuropathologists based on surgically resected material. The control group consisted of consented individuals who had a general medical exam at the Mayo Clinic. Matching variables were sex, date of birth (within two and one half years), self-identified race (Hispanic white, non-Hispanic white, American Indian, African American, Asian, Pacific Islander, Other) and residence. Geographic region of residence was matched in three zones based on the distance to the Mayo Clinic Rochester: Olmsted County; the rest of Minnesota, Wisconsin, Iowa, North Dakota and South Dakota; and the rest of the United States and Canada. Excluded were individuals under the age of 18 and those with a history of brain tumor. The Mayo Clinic case and control enrollment research protocol was approved by Mayo Institutional Review Board. These cases and controls were genotyped using Illumina 610Quad arrays.

Sample preparation and genotyping for replication phase and quality control. DNA was isolated from snap-frozen, buffy-coat samples using an AutoGenFlex STAR system (AutoGen) with Qiagen's FlexiGene DNA AGF3000 kit and AutoGen's blood DNA finishing kit. DNA was quantified using a

ND-1000 spectrophotometer (Thermo Scientific) and normalized to 50 ng/ μ l using 10 mM Tris HCl, 0.1 mM EDTA, pH 8.0 buffer (Teknova). Genotyping was performed using Illumina 610Quad SNP arrays (Illumina) according to the manufacturer's recommendations. Briefly, 200 ng of genomic DNA was amplified then fragmented. The fragmented DNA was hybridized on Illumina's Human 610-Quad BeadChip. Fluorescent labeling was performed by single-base extension using labeled nucleotides. The BeadChip was then scanned with Illumina's Bead Array Reader. Samples, including positive controls, were processed in a 96-well format.

We carried out allele calling using Illumina's Genotyping Module version 3.3.7 in BeadStudio version 3.1.3.0. We summarized concordance in interplate, intraplate and overall subject replicates to investigate potential genotyping error. Subject-level call rates were calculated and those subjects with call rates <0.9 were excluded from further analysis. Individual SNP call rates were summarized and SNPs with call rates <0.9 were excluded from the analysis. The minor allele frequency (MAF) was calculated for each SNP, and SNPs with MAF < 0.01 were excluded from further analysis. The above analyses were done on the complete set of data, and each analysis was repeated separately for each plate to investigate any potential plate effects. The overall Illumina subject call rate across all SNPs for Mayo Clinic cases and controls was 97.5 ± 0.02 (median 98.3; range 90.0–98.4). Inter- and intraplate replicate analysis was performed for the 13 SNPs summarized in Table 1. For all 13 SNPs, all inter- and intraplate replicates were identical.

Statistical methods for replication phase. The frequency distribution at each SNP locus was tested against the Hardy-Weinberg equilibrium (HWE) under the allele mendelian biallelic expectation using the χ^2 test. SNPs with HWE P values <0.001 for control subjects were excluded from the analysis. The principal component approach was implemented in EIGENSTRAT to determine whether there was any evidence of population stratification in the Mayo cases and controls^{3,27}. We used an additive logistic regression model for 0, 1 or 2 copies of the minor allele for candidate SNPs to investigate the association of glioma risk. Significant principal components from the population stratification analysis were included as covariates in the logistic regression models. Haplotype blocks were estimated using Haploview²⁶. The multiple SNP marker-disease association by estimated haplotype was evaluated using haplo.score (a software developed by the Mayo Clinic), which accounts for ambiguous linkage phase²⁸.

- Felini, M.J. *et al.* Reproductive factors and hormone use and risk of adult gliomas. *Cancer Causes Control* **20**, 87–96 (2009).
- Wrensch, M. *et al.* Nonsynonymous coding single-nucleotide polymorphisms spanning the genome in relation to glioblastoma survival and age at diagnosis. *Clin. Cancer Res.* **13**, 197–205 (2007).
- Davis, F.G. *et al.* Issues of diagnostic review in brain tumor studies: from the Brain Tumor Epidemiology Consortium. *Cancer Epidemiol. Biomarkers Prev.* **17**, 484–489 (2008).
- Pico, A.R. *et al.* SNPLoc: an interactive single nucleotide polymorphism selection, annotation, and prioritization system. *Nucleic Acids Res.* **37**, D803–D809 (2009).
- Dausset, J. *et al.* Centre d'étude du polymorphisme humain (CEPH): collaborative genetic mapping of the human genome. *Genomics* **6**, 575–577 (1990).
- Hung, R.J. *et al.* A susceptibility locus for lung cancer maps to nicotinic acetylcholine receptor subunit genes on 15q25. *Nature* **452**, 633–637 (2008).
- Barrett, J.C., Fry, B., Maller, J. & Daly, M.J. Haploview: analysis and visualization of LD and haplotype maps. *Bioinformatics* **21**, 263–265 (2005).
- Patterson, N., Price, A.L. & Reich, D. Population structure and eigenanalysis. *PLoS Genet.* **2**, e190 (2006).
- Schaid, D.J., Rowland, C.M., Tines, D.E., Jacobson, R.M. & Poland, G.A. Score tests for association between traits and haplotypes when linkage phase is ambiguous. *Am. J. Hum. Genet.* **70**, 425–434 (2002).